5. S. O'Gorman and G. M. Wahl, unpublished observations.
6. pOG44 consisted of the cytomegalovirus immediate-early promoter from pCDM8 (*18*), a 5′ leader sequence and synthetic intron from pMLSIScat (*13*), the FLP coding sequence [nucleotides 5568 to 6318 and 1 to 626 of the 2-μm circle (*15*)], and the SV40 late region polyadenylation signal from pMLSIScat (*13*). The following silent nucleotide substitutions were introduced into the structural FLP sequences with the use of the polymerase chain reaction: C for T at position 5791 (*15*), G for A at 5794, G for C at 5800, C for T at 55, G for A at 58, and C for T at 55, G for A at 58, and C for T at 103. These changes eliminated three canonical AATAAA polyadenylation signals and introduced a Pst I restriction site without altering the amino acids encoded by the sequence. These alterations did not appear to significantly affect the expression of FLP by mammalian cells. pOG28 consisted of a murine cDNA for dihydrofolate reductase (*6*) cloned into pCDM8.
7. R. J. Bollag, A. S. Waldman, R. M. Liskay, *Annu. Rev. Genet.* **23**, 199 (1989).
8. pOG45 consisted of the neomycin resistance cassette and 3′ FRT from pNEOβGAL cloned into pUC19. pOG45A was derived from pOG45 by deleting a 200-bp fragment containing the FRT.
9. J. F. Senecoff, P. J. Rossmeissl, M. M. Cox, *J. Mol. Biol.* **201**, 405 (1988).
10. B. Sauer and N. Henderson, *New Biologist* **2**, 441 (1990).
11. K. G. Golic and S. Lindquist, *Cell* **59**, 499 (1989).
12. B. Sauer and N. Henderson, *Nucleic Acids Res.* **17**, 147 (1989).
13. M. T. F. Huang and C. M. Gorman, *ibid.* **18**, 937 (1990).
14. S. M. Mount, *ibid.* **10**, 459 (1982).
15. J. L. Hartley and J. E. Donelson, *Nature* **286**, 860 (1980).
16. M. T. F. Huang and C. M. Gorman, *Mol. Cell. Biol.* **10**, 1805 (1990).
17. P. J. Southern and P. Berg, *J. Mol. Appl. Genet.* **1**, 327 (1982).
18. A. Aruffo and B. Seed, *Proc. Natl. Acad. Sci. U.S.A.* **84**, 8573 (1987).
19. U. Bond, *EMBO J. 7*, 3509 (1988).
20. H. J. Yost and S. Lindquist, *Cell* **45**, 185 (1986).
21. B. Hirt, *J. Mol. Biol.* **26**, 365 (1967).
22. F. L. Graham, J. Smiley, W. C. Russel, R. Nairn, *J. Gen. Virol.* **36**, 59 (1977).
23. F. L. Graham and A. J. van der Eb, *Virology* **52**, 456 (1973).
24. J. de Wet, K. V. Wood, M. DeLuca, D. R. Helenski, S. Subramani, *Mol. Cell. Biol. 7*, 725 (1987).
25. C. V. Hall, P. E. Jacob, G. M. Ringold, F. Lee, *J. Mol. Appl. Genet.* **2**, 101 (1983).
26. J. R. Sanes, J. L. R. Rubenstein, J.-F. Nicolas, *EMBO J.* **5**, 3133 (1986).
27. K. Thomas and M. Capecchi, *Cell* **51**, 503 (1987).
28. We thank M. McKeown, R. Heyman, and R. Evans for their insightful contributions to this work and the preparation of the manuscript. M. Jayaram provided the FRT and FLP coding sequences. Supported by Xerox Corporation, Bayer A. G., the Weingart Foundation, and the Mathers Foundation.

28 August 1990; accepted 8 January 1991

Multiple Representations of Pain in Human Cerebral Cortex

JEANNE D. TALBOT, SEAN MARRETT, ALAN C. EVANS, ERNST MEYER, M. CATHERINE BUSHNELL, GARY H. DUNCAN*

The representation of pain in the cerebral cortex is less well understood than that of any other sensory system. However, with the use of magnetic resonance imaging and positron emission tomography in humans, it has now been demonstrated that painful heat causes significant activation of the contralateral anterior cingulate, secondary somatosensory, and primary somatosensory cortices. This contrasts with the predominant activation of primary somatosensory cortex caused by vibrotactile stimuli in similar experiments. Furthermore, the unilateral cingulate activation indicates that this forebrain area, thought to regulate emotions, contains an unexpectedly specific representation of pain.

DESPITE THE POWERFUL NATURE OF pain as a sensation, there is little consensus regarding the involvement of the cerebral cortex in pain processing. Early this century, Head and Holmes (*1*) observed individuals with war injuries and concluded that the cerebral cortex played only a minimal role in pain perception. Penfield and Boldrey (*2*) reached a similar conclusion when they found that patients rarely reported a sensation of pain on electrical stimulation of their exposed cerebral cortex during surgery to remove epileptic seizure foci. Thus, a commonly held view in clinical neurology is that "stimulation of . . . any . . . cortical areas in a normal, alert human being does not produce pain" (*3*).

Other data indicate that several areas of the cerebral cortex may process nociceptive information. Some patients with epileptic foci involving the primary or secondary somatosensory areas of the parietal lobe (SI and SII, respectively) experience pain during seizures (*4*). In addition, lesions of these areas in humans can sometimes lead to reduced pain perception (*5*). Single neurons in both SI and SII of the parietal cortex of awake monkey respond to nociceptive stimuli (*6*); however, these findings are so rare that the functional significance of parietal nociceptors is still in question.

Frontal cortex has also been implicated in pain processing. In cat and in humans, noxious electrical stimuli induce an increase in cerebral blood flow to the frontal lobes (*7*). In rat there are neurons in the prefrontal cortex that respond to noxious skin stimulation (*8*). In addition, in patients resection of the anterior cingulate cortex can reduce the distress associated with chronic intractable pain (*9*). Nevertheless, the unreliable nature of this surgical procedure in relieving pain (*10*) and the absence of precise anatomical data from humans, uncompromised by disease or lesions, underscore our lack of knowledge concerning the normal function of specific cortical regions in pain processing.

We have now investigated the involvement of specific cortical areas in the perception of pain in awake, healthy, human volunteers. To functionally isolate the perception of pain from all other sensory and behavioral variables, we used subtractive positron emission tomography (PET). This technique can identify subtle differences in the activation of specific brain sites relative to sensory and evaluative processes (*11, 12*). In addition, we have applied methods (*13, 14*) that combine into stereotaxic images the functional information derived

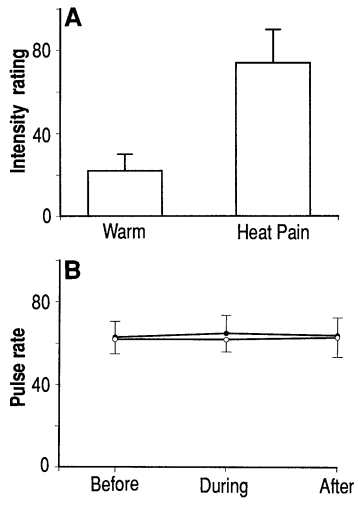

Fig. 1. (**A**) The perceived intensity of the thermal stimuli. Intensity ratings (mean ± SD) given by the eight subjects immediately after the PET scans in which the thermal stimuli were 41° to 42°C (Warm) or 47° to 49°C (Heat Pain). The ratings were different between the two conditions (paired t test, $t = 12.7$, $P < 0.0001$). (**B**) Mean pulse rate (±SD) of the eight subjects during 2-min epochs before, during, and after the termination of the PET scans during the Warm (○) and Heat Pain (●) conditions. A repeated-measures multivariate analysis of variance revealed no significant changes in pulse rate over time [$F(2) = 0.05$, $P = 0.95$] nor between the Warm and Heat Pain conditions [$F(1) = 0.73$, $P = 0.38$].

J. D. Talbot, M. C. Bushnell, G. H. Duncan, Laboratoire de neurophysiologie comportementale, Faculté de médecine dentaire, Université de Montréal, Montreal, Quebec, Canada H3C 3J7.
S. Marrett, A. C. Evans, E. Meyer, Positron Imaging Laboratories, McConnell Brain Imaging Center, Montreal Neurological Institute, Montreal, Quebec, Canada H3A 2B4.

*To whom correspondence should be addressed.

from PET with the anatomical information from magnetic resonance imaging (MRI), a procedure that allows direct identification of soft-tissue structures used in stereotaxic averaging and thus increases the precision of functional localizations.

Eight right-handed male subjects (25 to 31 years of age) underwent six to seven 60-s PET scans (*15*) within a single experimental session. During four of these scans, subjects received cutaneous heat stimuli; these data are described here. In each of the four scans, a series of 12 5-s heat pulses were delivered by a contact thermode (1 cm in diameter) to six spots on the subject's right volar forearm (*16*). During two scans, the stimuli consisted of a double heat pulse described as painful but tolerable (48° to 49°C), or "Heat Pain"; stimuli presented during the other two scans were described as clearly warm but not painful (41° to 42°C), or "Warm" (*17*). After each scan, subjects rated the intensity of the stimuli using a modified magnitude estimation scale (*18*) in which 50 was defined as just barely painful. Pulse rate was monitored before, during, and after each scan. Heat Pain and Warm conditions were presented in a pseudorandom manner with a period of at least 10 min between successive scans. So that anxiety associated with the painful stimuli would be minimized (and so that each subject's threshold for pain, pain tolerance, and withdrawal reflex could be determined), all subjects participated in a practice session several days before the PET scan experiments.

After completing the PET sessions, each subject underwent a high-resolution MRI head scan, which was subsequently used to align data sets stereotactically for within- and between-subject averaging of functional data (*19*). Localized changes in normalized cerebral blood flow (CBF) between the Heat Pain and Warm conditions were tested for significance with an automatic peak-detection algorithm and then displayed as a *t*-statistic image merged with the MRI and averaged across all subjects (*20*). Peaks with t values greater than 3.5 ($Z > 2.17$; $P < 0.03$) are reported as significant.

All subjects rated the noxious heat as clearly painful and the warm stimuli as below pain threshold (Fig. 1A). Nevertheless, subjects' pulse rates were within normal range and not significantly higher than during the warm stimulation (Fig. 1B), indicating that the stimuli did not produce significant anxiety or stress (*20*).

The painful stimulus produced four significant peaks of activity in the cerebral cortex (Table 1 and Fig. 2). In Fig. 2, the averaged MRI-PET volume was sliced horizontally at coordinates corresponding to local maxima of the significant peaks. The most prominent focus of pain-related activation (Table 1, peak 1, and Fig. 2C) approximated the border between the cingulum and the anterior cingulate gyrus (Brodmann's area 24). In addition, a secondary but significant peak (Table 1, peak 4, and Fig. 2B) was seen more posteriorly within area 24. Significant peaks of activation were also found deep in the parietal lobe along the upper bank of the lateral sulcus (Table 1, peak 2, and Fig. 2D), a location described as SII in humans and in monkey (*22*), and in the SI arm area of the postcentral gyrus (Table 1, peak 3, and Fig. 2A). All significant pain-related foci were restricted to the cortex contralateral to the stimulated arm.

Fig. 2. Cortical activation induced by a painful stimulus. Heat Pain minus Warm conditions, averaged from eight subjects (two scans per condition per subject), visualized with merged PET-MRI horizontal slices at superior-inferior coordinates (**A**) +60, (**B**) +39, (**C**) +33, and (**D**) +29. The degree to which individual sulci are distinguished in the average MRI indicates the accuracy achieved in matching functional and anatomical data from the eight subjects. The range of t values for PET data is coded by color (blue, $t = 3.2$; red-white transition, $t = 6.0$). Significant pain-related foci are restricted to the cortex contralateral to the stimulated arm: SI [(A), peak 3], anterior cingulate [(B), peak 4 and (C), peak 1], and SII [(D), peak 2]. Nonsignificant trends for possible bilateral activation of SII are seen in (C) and (D). (D) illustrates the strong contralateral activation of SII, deep in the lateral sulcus, as well as remnants of activation associated with the inferior extent of the anterior cingulate gyrus near the midline. The bridging between these two areas probably represents the limitations of the imaging system in spatially resolving these two strong foci.

The finding that both primary and secondary somatosensory cortical areas are activated by painful skin stimulation indicates that each of these regions is involved in the processing of heat pain information in humans. It is well established that single neurons within both areas are activated by innocuous mechanical stimuli (*6*); however, because the subtractive PET analysis eliminates activity attributable to factors common to both experimental conditions, the activation we observe in SI and SII is the result of the painful heat and not of the mechanical contact or innocuous warming of the skin. Because heat information is conveyed by two distinct populations of peripheral nerves—warm fibers, which respond maximally at temperatures less than 44°C, and heat nociceptors, which only begin to respond at 44°C (*23*)—the cortical activation related to painful heat stimuli most likely originates through activity of these nociceptive primary afferents. The strong pain-related activation of SII contrasts with the predominant activation of SI by nonpainful vibrotactile stimuli in similar experiments (*24*). Thus, at least two areas within the parietal lobe of the human cerebral cortex are activated by heat pain, and SII cortex may be more important for processing of pain than for processing of tactile information.

We observed a pronounced unilateral activation in the region of the anterior cingulate gyrus (area 24) related to heat pain. This area has been classified as part of the limbic system of the brain, which is thought to control emotions and affective responses to pain (*25*). Accordingly, neurosurgeons have resected this area (usually bilaterally) in cases of intractable pain with a strong emotional component and found that patients complained less about their pain but still acknowledged its existence (*9*). Nevertheless, a number of factors indicate that the anterior cingulate activation is not simply the result of emotional arousal or anxiety. First, general anxiety attributable to the experimental

Table 1. Significant pain-related foci of activation. Coordinates of peak activation are expressed in millimeters (*19*). M-L, medial-lateral relative to midline (positive = right); A-P, anterior-posterior relative to anterior commissure (positive = anterior); S-I, superior-inferior relative to commissural line (positive = superior). Probability (Prob.) estimates are based on *Z* scores (*20*).

Peak no.	Stereotaxic coordinates			Activation indices			Cortical area
	M-L	A-P	S-I	*t* statistic	*Z* score	Prob.	
1	−15	+1	+33	5.32	3.23	0.002	Ant. cingulate
2	−44	−23	+29	4.11	2.50	0.02	SII
3	−31	−31	+60	3.58	2.18	0.03	SI
4	−5	−17	+39	3.56	2.17	0.03	Ant. cingulate

situation is common to both the Heat Pain and Warm conditions and thus is eliminated by the data analysis. Second, subjects report that the stimuli evoke little emotional reaction; in fact, these stimuli are described as the least unpleasant of commonly used experimental pain stimuli (*26*). Third, the levels of noxious heat were determined for each subject to be painful but within his range of tolerance. Fourth, practice sessions were conducted so that the anxiety and emotional reactions associated with a novel experimental situation or unexpected noxious stimuli would be reduced; as a result, pulse rates were normal throughout the experimental procedures. Finally, a strictly emotional reaction to the stimuli would be expected to result from activation of nonspecific arousal pathways and to produce a bilateral activation of limbic structures (*25*).

In contrast to our results, human studies of anxiety (in anticipation of pain) reveal bilateral activation of several cortical sites, but not within or close to the cingulate gyrus (*27*).

An alternative explanation for the unilateral activation in the region of the anterior cingulate cortex is that this increased activity reflects encoding of the intensity and laterality of noxious stimuli. In the cat, area 24 receives an ipsilateral projection from the ventral border of the thalamic ventrobasal complex (*28*), an area that may be specifically nociceptive in humans (*29*). In addition, nociceptive neurons in the region of the thalamic centromedial (CM) and parafasicular (Pf) nuclei of monkeys have exquisite intensity-discriminative properties (*30*), and other evidence shows that CM and Pf project to the anterior cingulate cortex (*31*). Finally, data collected in a subset of the current subject population indicate that area 24 is selectively activated by the noxious thermal stimuli and not by innocuous touching or warming of the skin (*32*). These data, in conjunction with our current finding, suggest that information concerning both the intensity and laterality of noxious stimuli is relayed along pathways thought to have only an affective-motivational function (*33*). Encoding information about potentially dangerous stimuli is of teleological importance and may be a major role of paleolimbic pathways.

Thus, the normal processing of painful stimuli in humans is not distributed over large areas of the cortex, but is restricted to three major structures—anterior cingulate cortex, SII, and SI. We propose that precise information about pain intensity and laterality reaches both parietal and frontal cortical areas. This information may then contribute to the evaluation of temporal and spatial features of pain in the parietal area and to the regulation of emotional reactions in the limbic regions of frontal cortex.

REFERENCES AND NOTES

1. H. Head and G. Holmes, *Brain* **34**, 102 (1911).
2. W. Penfield and E. Boldrey, *ibid.* **60**, 389 (1937). The authors state, "pain [probably] has little, if any true cortical representation" (p. 441).
3. R. D. Adams and M. Victor, *Principles of Neurology* (McGraw-Hill, New York, 1989), p. 108.
4. G. B. Young, H. W. K. Barr, W. T. Blume, *Ann. Neurol.* **19**, 412 (1986); G. B. Young and W. T. Blume, *Brain* **106**, 537 (1983).
5. J. C. White and W. H. Sweet, *Pain and the Neurosurgeon: A Forty-Year Experience* (Thomas, Springfield, IL, 1969).
6. D. R. Kenshalo *et al.*, *Brain Res.* **454**, 378 (1988); C. J. Robinson and H. Burton, *J. Comp. Neurol.* **192**, 93 (1980); W. K. Dong *et al.*, *Brain Res.* **484**, 314 (1989).
7. T. Tsubokawa *et al.*, *Brain Res.* **217**, 179 (1981); N. A. Lassen *et al.*, *Sci. Am.* **139**, 62 (October 1978).
8. L. Mioche and W. Singer, *J. Neurophysiol.* **62**, 185 (1989); J. Mantz, C. Milla, J. Glowinski, A. M. Thierry, *Neuroscience* **27**, 517 (1988).
9. E. L. Foltz and E. W. Lowell, *J. Neurosurg.* **19**, 89 (1962); R. W. Hurt and H. T. Ballantine, Jr., *Clin. Neurosurg.* **21**, 334 (1973).
10. D. H. Wilson and A. E. Chang, *Confin. Neurol.* **36**, 61 (1974); J. L. Santo *et al.*, *Pain* **41**, 55 (1990).
11. M. Corbetta *et al.*, *Science* **248**, 1556 (1990); P. T. Fox *et al.*, *J. Neurosurg.* **67**, 34 (1987).
12. S. E. Petersen *et al.*, *Nature* **331**, 585 (1988).
13. A. C. Evans, C. Beil, S. Marrett, C. J. Thompson, A. Hakim, *J. Cereb. Blood Flow Metab.* **8**, 513 (1988).
14. A. C. Evans, S. Marrett, L. Collins, T. M. Peters, *Proc. SPIE—Int. Soc. Optical Eng.* **1092**, 264 (1989).
15. PET scans were obtained with the Scanditronix PC-2048B system, which produces 15 image slices at an intrinsic resolution of 5 by 5 by 6.5 mm [A. C. Evans, C. J. Thompson, S. Marrett, E. Meyer, M. M. Mazza, *IEEE Trans. Med. Imaging,* in press]. The relative distribution of CBF was measured during each scan with the bolus ^{15}O-labeled H_2O methodology without arterial blood sampling [P. T. Fox and M. A. Mintun, *J. Nucl. Med.* **30**, 141 (1989)]. We smoothed the images with a 20-mm Hanning filter to overcome residual anatomical variation (*34, 35*); C. J. Lueck *et al.*, *Nature* **340**, 386 (1989)].
16. The 5-s heat-pulse stimuli [M. A. Larson, J. G. McHaffie, B. E. Stein, *J. Neurosci.* 7, 547 (1987)] were presented consecutively to the six different spots of skin (3 cm by 2 cm grid, 4-cm minimum separation) so that tissue damage and sensitization would be avoided [D. D. Price, P. McGrath, A. Rafii, B. Buckingham, *Pain* **17**, 45 (1983)].
17. The double heat-pulse procedure maximizes neuronal responses to noxious heat and minimizes habituation [M. C. Bushnell and G. H. Duncan, *Exp. Brain Res.* **78**, 415 (1989); W. Maixner, R. Dubner, D. R. Kenshalo, Jr., M. C. Bushnell, J.-L. Oliveras, *J. Neurophysiol.* **62**, 437 (1989)]; temperatures chosen for the Heat Pain condition (seven subjects: 47° and 48°C; one subject: 48° and 49°C) were based on the subject's pain tolerance and withdrawal response; temperatures used for the Warm condition (six subjects: 41°C; two subjects: 42°C) were chosen on the basis of the subject's pain threshold.
18. J. C. Willer, A. Roby, D. Le Bars, *Brain* **107**, 1095 (1984); J. D. Talbot, G. H. Duncan, M. C. Bushnell, M. Boyer, *Pain* **30**, 221 (1987).
19. MRI scans (64 slices, 2-mm thick) were obtained from a Philips 1.5T Gyroscan and resliced so as to be in register with the PET data with a PIXAR three dimensional (3-D) computer (*14*) (A. C. Evans, S. Marrett, J. Torrescorzo, S. Ku, L. Collins, *J. Cereb. Blood Flow Metab.*, in press). We used interactive 3-D image software to establish an orthogonal coordinate frame based on the anterior commissure–posterior commissural line from the MRI image. These coordinates were used for linear resampling of each matched pair of MRI and PET data sets into a standardized stereotaxic coordinate system [J. Talairach and P. Tournoux, *Co-Planar Stereotaxic Atlas of the Human Brain* (Thieme, New York, 1988)].
20. PET images were normalized for global CBF and the image volume of the mean state-dependent change (ΔCBF) was obtained [P. T. Fox, J. S. Perlmutter, M. E. Raichle, *J. Comput. Assist. Tomogr.* **9**, 141 (1985)]. The ΔCBF volume was converted to a *t*-statistic volume by division of each voxel by the mean standard deviation in normalized CBF for all intracerebral voxels. Individual MRI images were subjected to the same averaging procedure, such that composite stereotactic image volumes (128 by 128 by 80 voxels in extent and sampled at approximately 1.5 mm in each dimension) were obtained for both the *t* statistic and MRI. We merged anatomical and functional images to allow direct localization on the MRI images of *t*-statistic peaks (*34*) and for the anatomical correlation of extended zones of activation not expressible in terms of isolated peaks. For the initial peak search, the *t*-statistic volume was filtered with a 7-pixel diameter spherical smoothing kernel and the stereotactic coordinates of local extrema in the smoothed volume recorded. The peak distribution was then searched for significant signals with change-distribution analysis (*35*) and *Z*-score thresholding (*12*). This procedure identified the *Z*-score and corresponding *t* statistic used to establish a threshold for visualizing the *t* image at a selected *P* value.
21. G. E. Deane, *J. Exp. Psychol.* **61**, 489 (1961).
22. W. Penfield and H. Jasper, *Epilepsy and the Functional Anatomy of the Human Brain* (Little, Brown, Boston, 1954), pp. 77–78; C. J. Robinson and H. Burton, *J. Comp. Neurol.* **192**, 93 (1980).
23. R. Duclaux and D. R. Kenshalo, Sr., *J. Neurophysiol.* **43**, 1 (1980); H. Hensel and A. Iggo, *Pfluegers Arch.* **329**, 1 (1971); R. Sumino and R. Dubner, *Brain Res. Rev.* **3**, 105 (1981).
24. P. T. Fox, H. Burton, M. E. Raichle, *J. Neurosurg.* **67**, 34 (1987); (*35*).
25. P. D. MacLean, *Psychosom. Med.* **11**, 338 (1949); J. W. Papez, *Arch. Neurol. Psychiatry* **38**, 725 (1937); B. A. Vogt, D. L. Rosene, D. N. Pandya, *Science* **204**, 205 (1979).
26. When stimulus levels are equated for perceived intensity, phasic noxious stimuli such as heat pulses evoke less of an affective reaction from subjects than do tonic noxious stimuli such as immersion of the hand in cold water or ischemia [P. Rainville *et al.*, *Am. Pain Soc. Abstr.* **8**, 64 (1989)].
27. E. M. Reiman, M. J. Fusselman, P. T. Fox, M. E. Raichle, *Science* **243**, 1071 (1989).

28. Y. Yasui, K. Itoh, H. Kamiya, T. Ino, N. Mizuno, *J. Comp. Neurol.* **274**, 91 (1988).
29. J. R. Dostrovsky, R. R. Tasker, S. E. B. Wells, L. Lee, paper presented at the Symposium on Neurobiology of Nociception, Kawai, HI, 9 to 12 April 1990.
30. M. C. Bushnell and G. H. Duncan, *Exp. Brain Res.*, in (*17*).
31. S. Y. Musil and C. R. Olson, *J. Comp. Neurol.* **272**, 203 (1988).
32. PET data from a no-stimulation "Baseline" condition were collected for six subjects (in addition to data from the Heat Pain and Warm conditions). Subtractive analysis of Warm minus Baseline revealed no tendency ($t = -0.70$) toward activation at or near the prominent anterior cingulate focus observed with the Heat Pain condition.
33. R. Melzack and K. L. Casey, *The Skin Senses*, D. R. Kenshalo, Sr., Ed. (Thomas, Springfield, IL, 1968), pp. 423–443.
34. M. A. Mintun, P. T. Fox, M. E. Raichle, *J. Cereb. Blood Flow Metab.* **9**, 96 (1989).
35. P. T. Fox *et al.*, *ibid.* **8**, 642 (1988).
36. We thank the staff of the McConnell Brain Imaging Centre, the Medical Cyclotron Unit, and the Neurophotography Department for their technical assistance, and A. Gjedde and J. Lund for comments on the manuscript. Special thanks to P. Neelin, L. Collins, G. Filosi, and G. Lambert for technical assistance. Supported by Canadian Medical Research Council, the Isaac Walton Killam Fellowship Fund of the Montreal Neurological Institute, and the McDonnell-Pew Foundation.

5 October 1990; accepted 4 January 1991

Movement of Neural Activity on the Superior Colliculus Motor Map During Gaze Shifts

DOUGLAS P. MUNOZ,* DENIS PÉLISSON,† DANIEL GUITTON‡

The superior colliculus contains neurons that cause displacements of the visual axis (gaze shifts). These cells are arranged topographically in a motor map on which the vector (amplitude and direction) of the coded movement varies continuously with location. How this spatial representation becomes a temporal code (frequency and duration) in the motoneurons is unknown. During a gaze shift, a zone of neural activity moved continuously on the map from an initial location, defining the vector of the desired gaze shift, to a final "zero" position containing neurons that were active during fixation. Thus, the spatial-temporal transformation may be accomplished by control of gaze throughout the spatial trajectory of activity on the motor map.

THE MAMMALIAN SUPERIOR COLLICULUS (SC) is a laminated neural structure that transforms sensory information into motor commands that rapidly move the visual axis (*1*). Visually responsive neurons in the superficial layers are organized into a retinotopic map of visual space, subtending up to 80° of the contralateral visual field (*2*). Here we investigated the deeper layers, which are organized into a motor map (*1*).

In the cat, the animal studied here, coordinated eye-head movements are used to look at targets situated farther than about ±10° from center (*3*). Microstimulation of the deeper layers, in the cat whose head is unrestrained, elicits topographically coded gaze (gaze = eye-in-space = eye-in-head + head-in-space) shifts in which the vectors are predicted by the location being stimulated on the motor map (*4*). This motor map is retinotopically coded and is in spatial register with the overlying visual map.

The deeper layers contain tectoreticular neurons (TRNs) that control gaze shifts via projections to contralateral brainstem regions that generate eye and head movements (*5*). TRNs have both multimodal sensory responses (*6*) and movement-related discharges (*7–9*). Many TRNs burst just before a gaze shift. These neurons are grouped on the motor map into a large, nearly circular zone, the center of which specifies the amplitude and direction of the intended gaze shift. Other TRNs, located in the zero-amplitude location at the rostral pole of the SC, are active when the cat fixates a target and are silent during orienting gaze shifts (*8, 10*). Therefore, the retinotopic position of the ensemble of active TRNs differs if measured at the start and end of a gaze shift. In our experiments, we determined, in the cat, the retinotopic location of the active ensemble of neurons during a gaze shift (*11*).

We analyzed the activity of TRNs identified on the basis of their antidromic response after stimulation of the contralateral predorsal bundle (*7, 8*). The animal was required to make predictive gaze shifts to a spatial locus devoid of a newly appearing sensory cue, a procedure that prevented phasic visual responses from contaminating the movement-related neuronal activity.

The movement-related discharges of two TRNs, cells Q24 and Q37, recorded in the same cat are shown in Fig. 1. Of the two

Montreal Neurological Institute, Department of Neurology and Neurosurgery, McGill University, 3801 University, Montréal, Québec, Canada H3A 2B4.

*Present address: Laboratory of Sensorimotor Research, National Eye Institute, National Institutes of Health, Building 10, Room 10c101, Bethesda, MD 20892.
†Present address: Vision et Motricité, INSERM, U-94, 16 avenue du Doyen Lepine, 69500 Bron, France.
‡To whom correspondence should be addressed.

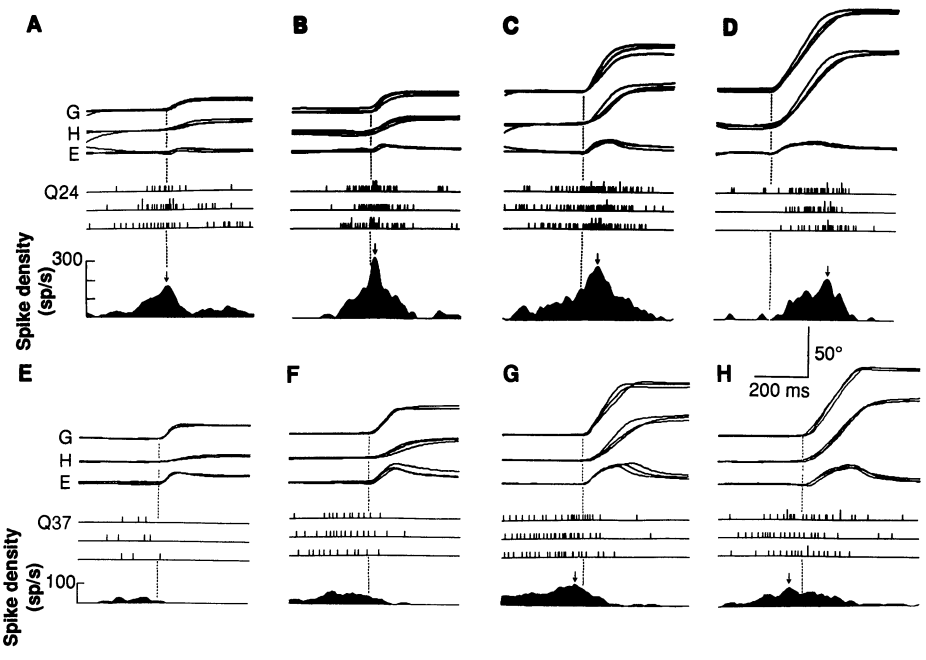

Fig. 1. Movement-related discharges of TRNs. Shown in each panel are the gaze (G), head (H), and eye (E) position traces; neural discharge for cells Q24 (**A** to **D**) and Q37 (**E** to **H**); and spike density function [number of action potentials (spikes) per second (sp/s)] (*11*). The occurrence of an action potential is represented by a small vertical line. Additional small lines superimposed on top of others indicate extra spikes within the same 2-ms time bin. The preferred movements for cell Q24 were directed horizontally and for cell Q37 were directed down to the left at an angle of about 45° to the horizontal. Traces are aligned on gaze-shift onset (vertical dashed lines). Arrows, maximum spike density.